A new model for describing the behaviour of soft soils under cyclic loading

B Indraratna[1]; J Ni[2]; C Rujikiatkamjorn[3]; and R Zhong[4]

[1]Professor of Civil Engineering, Director, Centre for Geomechanics and Railway Engineering, School of Civil, Mining and Environmental Engineering, University of Wollongong, Wollongong City, NSW 2522, Australia; PH (61) 2 42213046; FAX (61) 2 42213238; email: indra@uow.edu.au
[2]Lecturer, Dept. of Civil Engineering, Univ. of Shanghai for Science and Technology, 516 Jungong Road, 200093 Shanghai, P. R. China; email: wendy_1943@163.com
[3]Associate Professor, Centre for Geomechanics and Railway Engineering, School of Civil, Mining and Environmental Engineering, University of Wollongong, Wollongong City, NSW 2522, Australia; PH (61) 2 42215852; FAX (61) 2 42213238; email: cholacha@uow.edu.au
[4]Associate Research Fellow, Centre for Geomechanics and Railway Engineering, University of Wollongong, Wollongong City, NSW 2522, Australia; PH (61) 2 42213385; email: rzhong@uow.edu.au

ABSTRACT

Cyclic loading induced foundation instabilities such as the loss of bearing capacity and excessive plastic deformation of the subgrade are among the major concerns for the design and construction of transport infrastructure. There are limited studies on the modelling of cyclic loading of soft soils due to its complexities compared to static loading. In this study, a new constitutive model for soft clays under undrained cyclic triaxial loading has been developed based on the Modified Cam-clay theory. A new yield surface for elastic unloading was introduced by adopting two additional cyclic degradation parameters, which govern the change of the yield surface when unloading. Based on the proposed model, a numerical model is introduced to determine the effective stresses and strains. The proposed model was validated using the results of a series of undrained cyclic triaxial loading tests on kaolin. A good agreement between the numerical prediction and the measured excess pore pressures and axial strains was obtained. Furthermore, the factors which influence the cyclic performance of soft soils, e.g. the frequency, cyclic stress ratios and anisotropic consolidation stress, were investigated. The critical cyclic stress ratio can also be predicted by using the proposed model in terms of the excess pore pressures and axial strains. This theory was then applied to the combined vertical and radial consolidation of soft soils under cyclic loading, which represents the application of partially penetrated vertical drains for road and rail infrastructure at soft soil sites for a rail project in Sandgate, NSW. The objective of the partially penetrated drain within this 30 m deep estuarine soil was to consolidate the shallow soft clay layer underneath the track.

Keywords: cyclic loading, soft clays, cyclic degradation, cyclic stress ratio, combined vertical and radial consolidation, vertical drains

1 INTRODUCTION

Under cyclic loading, the excess pore pressures and strains of soft soils increase with the increasing number of cycles. This makes the accumulation of excess pore pressure and excessive plastic deformation of the subgrade a major concern for highway pavements, railway tracks and airport runways under significant cyclic loadings. Experimental studies in the past few decades have investigated the factors which influence the cyclic performance of soft soils, such as the cyclic stress level, loading frequency, over-consolidation ratio, and static pre-shearing (Larew and Leonards 1962; Takahashi et al. 1980; Sangrey et al. 1969; and Seed and Chan 1966). Cyclic models have been developed based on laboratory test data (Procter and Khaffaf 1984; Ansal and Erken 1989), but most of them have obvious shortcomings due to the simplified empirical assumptions or hypotheses. Although general constitutive models (Ramsamooj and Alwash 1990; Li and Meissner 2002) are considered to be more desirable, they are often too complex due to the required parameters which cannot be determined directly by conventional equipment.

Carter et al. (1980, 1982) proposed a practical model based on the Modified Cam-clay theory (Roscoe and Burland 1968), in which only one additional parameter was added into the latter to characterize the cyclic behaviour, and that parameter could be conveniently determined by cyclic triaxial loading tests. However, according to this model, the generation rate of excess pore pressure can increase

until the soil ultimately fails, which is in contrast to some of the previously reported tests (Takahashi et al. 1980; Miller et al. 2000; Zhou and Gong 2001; and Sakai et al. 2003). In this paper, a new cyclic model was developed, in which another additional degradation parameter was supplemented to overcome this shortcoming. Finally, this model was applied to combined vertical and radial consolidation of soft soils under cyclic loading at a railway site in Sandgate, NSW, Australia.

2 NEW CONSTITUTIVE CYCLIC MODEL

2.1 Contraction of the yield surface

Under repeated unloading-reloading process, the permanent excess pore pressures and strains of saturated soft clays often continue to increase. This phenomenon cannot be explained by the Modified Cam-clay model, but could be interpreted as the change of the yield surface by unloading. Assuming that the shape of the yield surface keeps unchanged, a cyclic parameter θ^* is introduced to indicate the contraction of the yield surface when the soil is elastically unloaded (Carter et al. 1980, 1982):

$$\frac{\mathrm{d}p_{\mathrm{c}}^{'}}{p_{\mathrm{c}}^{'}} = \theta^* \frac{\mathrm{d}p_{\mathrm{y}}^{'}}{p_{\mathrm{y}}^{'}} \tag{1}$$

where, $p_{\mathrm{c}}^{'}$ is a hardening parameter which could be considered as the pre-consolidation pressure, while $p_{\mathrm{y}}^{'}$ is a variable defined as (Roscoe and Burland 1968):

$$p_{\mathrm{y}}^{'} = p^{'} + \left(\frac{q}{M}\right)^2 \frac{1}{p^{'}} \tag{2}$$

In the above, M is the slope of the critical state line in $p'-q$ space, where p' and q are the effective mean stress and deviator stress.

In the proposed model, the parameter θ^* in Eq. (1) is assumed to decrease with the increasing number of cycles, N, rather than being constant, hence,

$$\theta^* = \frac{1}{\xi_1 N + \xi_2} \tag{3}$$

Where, ξ_1 and ξ_2 are empirical constants which can be determined experimentally.

2.2 Effective stresses and strains

The stress path for normally and isotropically consolidated soils under cyclic loading is shown in Fig. 1, in which $p'_{\mathrm{cl},i}$ (i=1, 2……, n) is the yield stress after the loading part of each cycle, $p'_{\mathrm{cu},i}$ (i=1, 2……, n) is the yield stress after the unloading part of each cycle, and $p'_{\mathrm{y},i}$ (i=1, 2……, n) is the loading parameter after each cycle.

In the first loading period, when the stress path moves from point A' to point A, excess pore pressure increases while the effective mean stress decreases. The yield stress corresponding to point A ($p'_{\mathrm{cl,1}}$) can be determined by Eq. (2), where the deviator stress at point A equals the cyclic stress q_{cyc}, and the effective mean stress is given by:

$$\frac{p_A^{'}}{p_{A'}^{'}} = \left(\frac{M^2 + \left(q_A / p_A^{'}\right)^2}{M^2 + \left(q_{A'} / p_{A'}^{'}\right)^2}\right)^{\frac{\lambda-\kappa}{\lambda}} \tag{4}$$

where λ and κ are the slopes of the normal compression and swelling lines respectively in $e-\ln p'$ space.

During the unloading period, the stress path travels from point A to A^*, and the effective mean stress remains constant. p'_{y1} is the loading parameter corresponding to point A^*. Based on Eq. (1), the yield stress for the second cycle or the yield stress after unloading can be calculated as:

$$p_{\mathrm{cu,1}}^{'} = p_{\mathrm{cl,1}}^{'}\left(\frac{p_{\mathrm{y,1}}^{'}}{p_{\mathrm{cl,1}}^{'}}\right)^{\theta^*} \tag{5}$$

In the first stage of the second cycle ($q<q_{\text{yielding}}$), where the yielding stress $q_{yielding}$ can be calculated by Eq. (2) with $p^{'} = p^{'}_{\text{y,1}}$ and $p^{'}_{\text{y}} = p^{'}_{\text{cu,1}}$, the stress path travels from point A^{*} to point B' and the soil behaves elastically. Afterwards, in the second stage for $q_{\text{yielding}}<q<q_{\text{cyc}}$ where q_{cyc} is the cyclic stress, the stress path moves from point B' to B, and the effective mean stress decreases, while the soil behaves plastically.

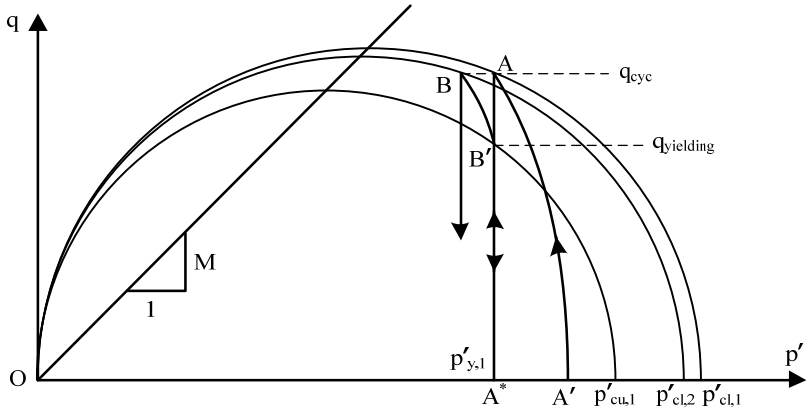

Figure 1. The stress path for cyclic loading

3 VALIDATION OF THE NEW MODEL

Undrained cyclic triaxial loading tests were carried out on the samples of reconstituted and saturated kaolin-water mixture using a triaxial loading apparatus. The cyclic stress ratio was defined as the ratio of cyclic stress to the maximum deviator stress at failure ($\text{CSR} = q_{\text{cyc}} / s_{\text{u0}}$). The latter was obtained through the conventional monotonic triaxial tests. A selection of the test conditions are given in Table 1.

Table 1: Test conditions and results

Sample	Mean effective stress after consolidation (P'_{c0}), kPa	Cyclic loading frequency (f), Hz	Cyclic stress ratio (CSR)	Loading cycles (N)	Failed or not	ξ_1	ξ_2
U_{02}	30	1	0.4	34,466	No	2.7	280
U_{06}	30	1	0.6	34,466	No	2.7	280
U_{10}	30	1	0.8	10,419	Yes	2.7	280
U_{03}	30	2	0.4	34,466	No	2.7	400
U_{07}	30	2	0.6	34,466	No	2.7	400
U_{11}	30	2	0.8	18,537	Yes	2.7	400

To validate the new cyclic model, comparisons were made between its predictions and the results of the above tests. Table 2 provides the parameters of soils properties and initial states, while the cyclic loading parameters ξ_1 and ξ_2 are given in Table 1, which indicates that ξ_2 increases with an increasing loading frequency.

Table 2: Parameters for soil properties and initial states

Soil properties				Initial states		
λ	κ	M	$p^{'}_{\text{c0}}$ (kPa)	$p^{'}_{0}$(kPa)	q_0(kPa)	e_0
0.18	0.03	1.68	30	30	16	1.32

The variation of normalized excess pore water pressure and axial strain with number of cycles are given in Fig. 2. A good agreement can be observed between the predicted results and the experimental trends. When CSR=0.8, the failure of specimen is observed for both f=1 and 2 Hz, as N exceeds 10,000 and 15,000, respectively. This state of failure is characterized by a rapid rise of axial strain beyond the critical value of N.

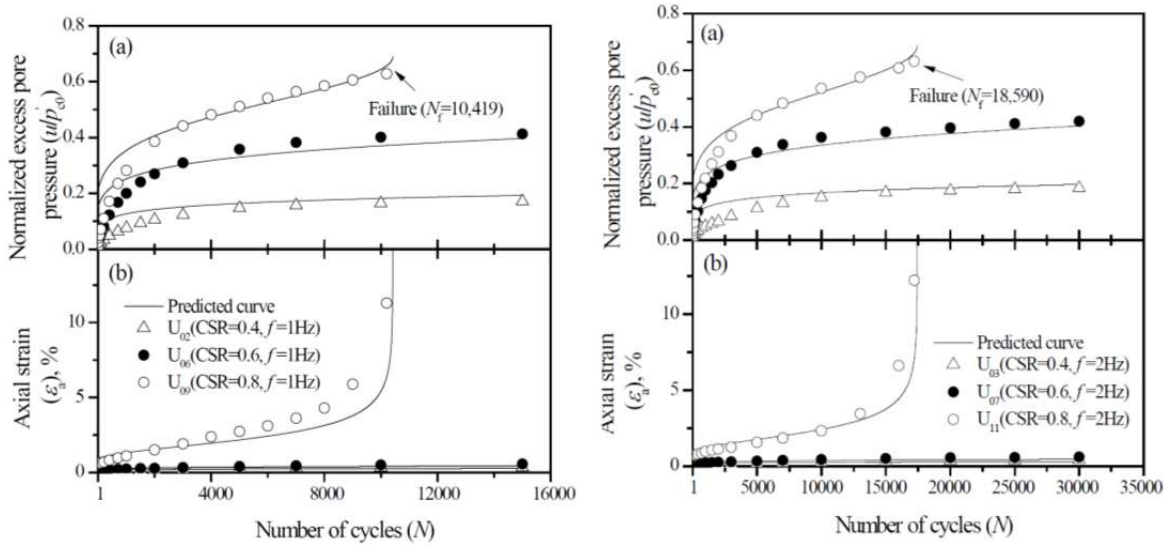

Figure 2. Predictions of excess pore pressures and axial strains: (a) f=1Hz, (b) f=2Hz

4 PARAMETRIC STUDY

In this section, the key parameters on the development of excess pore pressure and axial strains are investigated with a parametric study, for which the basic soil properties are given in Table 3.

Table 3: Parameters for undrained model analysis (Ni et al., 2014, with permission from ASCE)

λ	κ	M	p'_{c0} (kPa)	p'_0 (kPa)	e_0	G
0.25	0.05	1.2	30	30	0.6	$200s_{u0}$

Note: $s_{u0} = p'_{c0}(M/4)\left(2p'_0/p'_{c0}\right)^{\kappa/\lambda}$

4.1 Effect of CSR

The normalised excess pore pressures and axial strains calculated by the proposed model at various CSRs are given in Fig. 3. The results in Fig. 3(a) indicate that a critical state exists in an intermediate value of cyclic stress ratio (around 0.5 for this case). For larger CSR, the excess pore pressure increases so fast that the value of u_f / p'_{c0} (where u_f is the excess pore pressure at failure) reaches a high value in the first few cycles. When CSR is smaller than the critical cyclic stress ratio, the rates of excess pore pressure generation decrease and the specimens reach a stable state after an initial stage of rapid pore pressure development. Such a critical cyclic stress ratio can also be observed in Fig. 3(b) indicating two distinct observations, i.e. failure of specimens associated with a rapid increase in ε_a, and the attainment of a stable state at lower values of CSR<0.40.

4.2 Effect of Anisotropic Consolidation Stress Ratio

The results under various initial anisotropic consolidation stress ratios ($k_0 = \sigma'_{3c} / \sigma'_{1c}$) are given in Fig. 4. The soft soil behaves in a stable manner under cyclic loading at relatively large values of k_0 (0.8, 0.9, and 1.0). When k_0 drops to 0.7, the excess pore pressure and axial strain build up significantly, and the failure occurs around 400 cycles. With a smaller anisotropic consolidation stress ratio (k_0=0.6), the soil fails within fewer cycles (around 100 cycles). Hence, the anisotropic consolidation stress ratio k_0 plays an important role in predicting the behaviour of soft clays subjected to cyclic loading. The increasing rates of the excess pore pressure and axial strain decrease as the consolidation stress ratio increases. A stable state can be reached at a relatively large value of k_0, while failure would occur when k_0 is small, and also the number of cycles at failure decreases with a decreasing value of k_0.

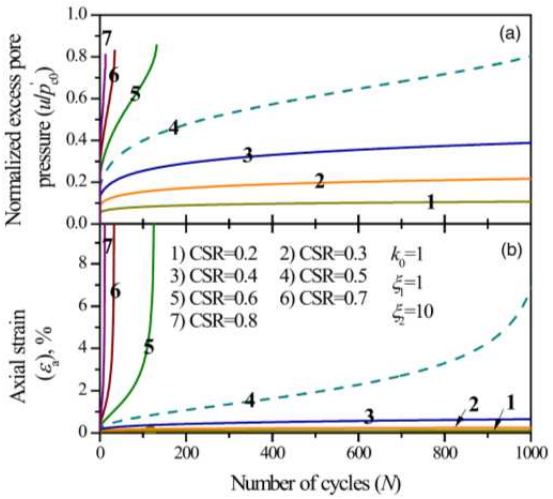

Figure 3. Predictions of the proposed model with different CSRs ($k_0 = 1$, $\xi_1 = 1$, $\xi_2 = 10$) (Ni et al., 2014, with permission from ASCE)

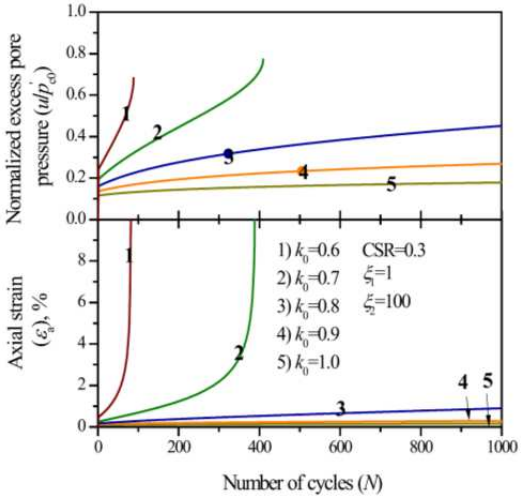

Figure 4. Predictions of the proposed model with different anisotropic consolidation stress ratios (CSR=0.3, ξ_1=1, ξ_2=100) (Ni et al., 2014, with permission from ASCE)

5 APPLICATION TO A CASE STUDY

5.1 Sandgate Rail Grade Separation Project

The Sandgate Rail Grade Separation Project was located at Sandgate, between Maitland and Newcastle, in the lower Hunter Valley of New South Wales, Australia. This project was the result of Kooragang Island becoming a major export terminal, where the coal trains need to cross the main lines at Sandgate to enter Kooragang Island.

The proposed model is utilized to compare the observed field data of this project. Due to the stringent time constraints placed on this project, only an initial train load at very low speed was considered to be the external surcharge instead of preloading with a conventional surcharge embankment. The installation of PVDs was chosen as a useful technique to effectively accelerate the dissipation of excess pore pressure, curtail the excessive lateral displacement, thus enhance the stability of the newly constructed (0.3 m high) rail track. The PVDs were determined to be 8 m long because the train load was generally restricted to a depth of 6-8 m, and the objective was to stabilize the relatively shallow soft clay layer beneath the crust, rather than the entire depth of soft clay (>30m depth).

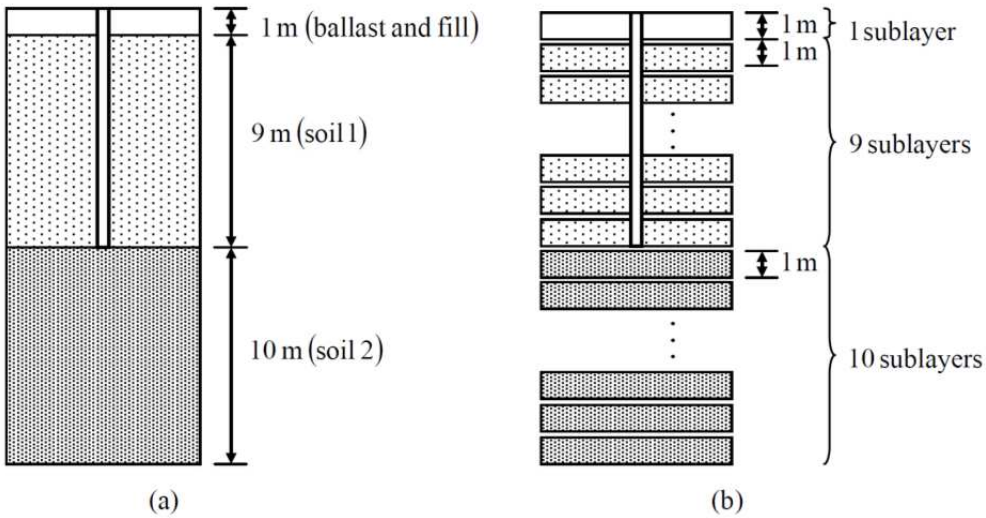

Figure 5. Unit cell with combined vertical and radial consolidation: (a) Three layers of the formation, (b) Sub-layers.

5.2 Soil parameters and loading condition

A soil cylinder with a combined vertical and radial consolidation under equal strain conditions was considered. The soil was divided into three layers, namely, ballast and fill, Soil 1, and Soil 2. Each layer can then be further divided into several sub-layers, as shown in Fig. 5. The parameters obtained from oedometer test, field vane shear test, and CPTU test for each layer of soil are given in Table 4.

Table 4: Parameters for fill and Soil layers at Sandgate Rail Grade Separation

	Sub-layer	Sub-layer thickness (m)	k_v (10^{-4}m/day)	k_h (10^{-4}m/day)	C_c	C_s	p_0' (kPa)	p_{c0}' (kPa)	e_0
Ballast and fill	1	1	0.7	1.4	0.91	0.105	6.2	15.49	2.26
Soil 1	2	1	0.7	1.4	0.92	0.11	11.99	29.98	2.26
	3	1	0.7	1.4	0.93	0.115	17.78	44.46	2.26
	4	1	0.7	1.4	0.94	0.12	23.58	58.94	2.26
	5	1	0.7	1.4	0.95	0.125	29.37	73.43	2.26
	6	1	0.7	1.4	0.96	0.13	35.16	87.91	2.26
	7	1	0.7	1.4	0.97	0.135	40.96	90.1	2.26
	8	1	0.7	1.4	0.98	0.14	46.75	88.83	2.26
	9	1	0.7	1.4	0.99	0.145	52.54	84.07	2.26
	10	1	0.7	1.4	1	0.15	58.34	75.84	2.26
Soil 2	11	1	0.75	1.5	1	0.15	64.34	64.34	2.04
	12	1	0.75	1.5	1.01	0.155	70.54	71.95	2.04
	13	1	0.75	1.5	1.02	0.16	76.74	79.81	2.04
	14	1	0.75	1.5	1.03	0.165	82.95	87.92	2.04
	15	1	0.75	1.5	1.04	0.17	89.15	96.28	2.04
	16	1	0.75	1.5	1.05	0.175	95.36	104.9	2.04
	17	1	0.75	1.5	1.06	0.18	101.56	113.75	2.04
	18	1	0.75	1.5	1.07	0.185	107.76	122.85	2.04
	19	1	0.75	1.5	1.08	0.19	113.97	132.2	2.04
	20	1	0.75	1.5	1.09	0.195	120.17	141.8	2.04

For Australian standard gauge operations (longitudinal distance between adjacent wheels is 2.02 m and the width between the rails is 2.55 m), the ratio of the speed of the train (km/h) to corresponding frequency is approximately 7 Hz. Therefore 5 Hz typically simulates the loading frequency of a cyclic load in the subgrade at a train speed of less than 40 km/h. The maximum amplitude of the cyclic load conforms to 25 tonne axle loads.

5.3 Comparison of observed and predicted settlement and lateral displacement

A comparison of the settlement at the centre line of the rail tracks between the predicted and field data is shown in Fig. 6. The predicted settlement agrees well with the measured data. The variation in the time-dependent settlement at different drain spacing is shown in Fig. 7. It is observed that 90% consolidation due to PVDs may be encountered within 1 year, whereas it will take much longer to achieve the same degree of consolidation without PVD.

The variation of in situ lateral displacement after 180 days at the toe of the rail embankment is presented in Fig. 8. As expected, maximum displacements were measured within the top layer of clay, i.e., the softest soil below the 1 m crust. As expected, lateral displacement was restricted to the topmost compacted fill (0-1 m deep). The predicted lateral displacement agrees well with the measurements. A comparison of lateral displacement at the 2.0 and 1.5 m drain spacing is given in Fig. 9, where the condition of no PVDs is also presented. In terms of excess pore pressure dissipation, little advantage was gained by a closer drain spacing of 1.5 m compared to a spacing of 2.0 m. As anticipated, the lateral displacements are shown to be at their maximum within the layer of soft clay directly beneath the compacted crust, about 1 m in thickness. Lateral displacement at 180 days may be as large as 0.04 m at a depth of around 1.0 m below the surface, however, the PVDs decrease the lateral movements by 25–35% depending on the drain spacing.

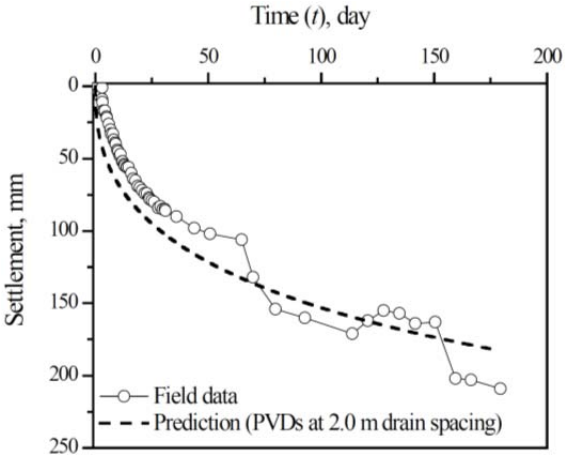

Figure 6. Comparison of settlements at the centre line of rail tracks between the predictions and field data

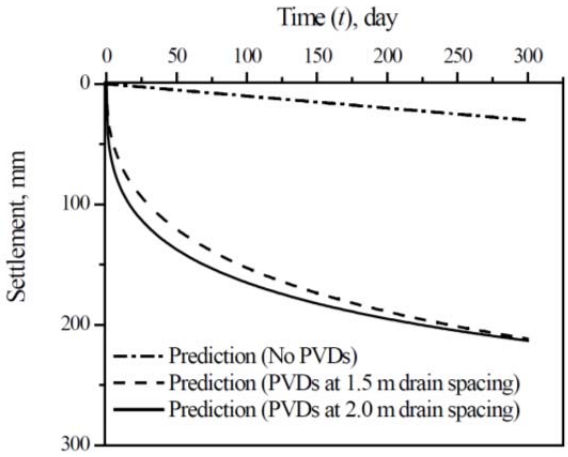

Figure 7. Surface settlements at the centre line of the rail load

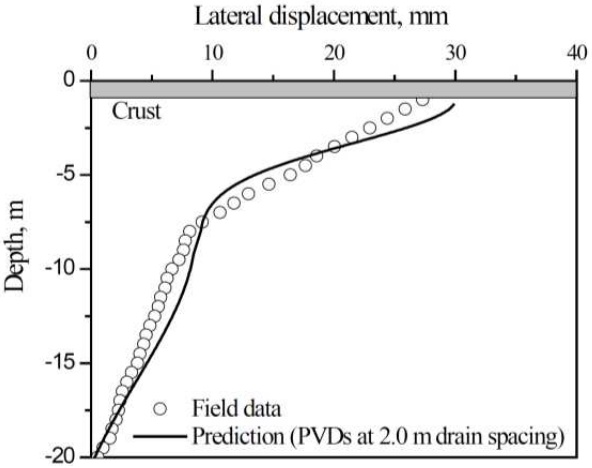

Figure 8. Comparison of lateral displacement near the rail embankment toe at 180 days between predictions and field data

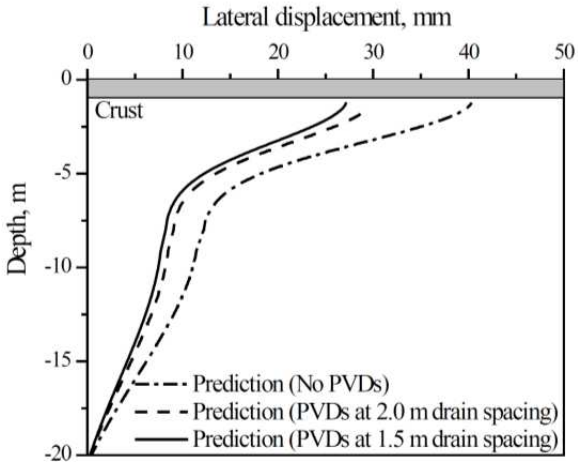

Figure 9. Lateral displacement profiles near the toe of the embankment at 180 days

6 CONCLUSIONS

A new cyclic model to simulate the behaviour of soft soils under repeated loading was proposed in this paper extending that of Carter et al. (1980, 1982). In the proposed model, only two additional cyclic degradation parameters (ξ_1 and ξ_2) were needed together with the traditional modified Cam-clay parameters, which could be determined from undrained cyclic triaxial tests. The parametric study shows that CSR and anisotropic consolidation stress ratio have strong impactions on the development of excess pore pressures and axial strains, and a stable state could be reached with relatively small value of the former and large value of the latter. The application of this theory to combined vertical and radial consolidation of soft soils under cyclic loading at a rail project in Sandgate, NSW indicated that the predictions of the proposed model agreed well with the field data.

7 ACKNOWLEDGEMENTS

The authors acknowledge the support of Australian Research Council (ARC), Innovative Research Project of Shanghai Municipal Education Commission (Project No. 14YZ081), and Young Teacher Training Scheme of Shanghai Municipal Education Commission (Project No. slg13027), for funding of

this research. The salient features of the paper have been published in the International Journal of Geomechanics, ASCE (Ni et al. 2014) with kind permission to be included in the paper.

REFERENCES

Ansal, A. M., and Erken, A. (1989). “Undrained hehavior of clay under cyclic shear stresses.” J. Geotech. Eng., 115(7), 968–983.

Carter, J. P., Booker, J. R., and Wroth, C. P. (1980). “The application of a critical state soil Model to cyclic triaxial tests.” Proc., 3rd Australia-New Zealand Conf. Geomech., Wellington, N.Z., 2, 121–126.

Carter, J. P., Booker, J. R., and Wroth, C. P. (1982). “A critical state soil model for cyclic loading.” Soil mechanics-transient and cyclic loading, Chichester: John Wiley & Sons, 219–252.

Larew, H. G., and Leonards, G. A. (1962). “A strength criterion for repeated loads.” Highway Research Board Proceedings, 41, 529–556.

Li, T., and Meissner, H. (2002). “Two-surface plasticity model for cyclic undrained hehavior of clays.” J. Geotech. Geoenviron. Eng., 128(7), 613–626.

Miller, G. A., Ten, S. Y., and Li, D. (2000). “Cyclic shear strength of soft railroad subgrade.” J. Geotech. Geoenviron. Eng., 126(2), 139–147.

Ni, J., Indraratna, B., Geng, X. Y., Carter, J. P. and Chen, Y. L. (2014). Model of soft soils under cyclic loading. International Journal of Geomechanics, online.

Procter, D. C., and Khaffaf, J. H. (1984). “Cyclic triaxial tests on remoulded clays.” J. Geotech. Engrg., 110(10), 1431–1445.

Ramsamooj, D. V., and Alwash, A. J. (1990). “Model prediction of cyclic response of soils.” J. Geotech. Engrg., 116(7), 1053–1072.

Roscoe, K. H., and Burland, J. B. (1968). “On the generalized stress–strain hehaviour of ‘wet’ clay.” Engineering Plasticity, Cam-bridge University Press, 535–609.

Sakai, A., Samang, L., and Miura, N. (2003). “Partially-drained cyclic hehavior and its application to the settlement of a low embankment road on silty-clay.” Soil Found., 43(1), 33–46.

Sangrey, D. A., Henkel, D. J., and Esrig, M. I. (1969). “The effective stress response of a saturated clay soil to repeated loading.” Can. Geotech. J., 6, 241–252.

Seed, H. B., and Chan, C. K. (1966). “Clay Strength under Earthquake Loading Conditions.” Proc. Amer. Soc. Civil Eng. vol. 92, SM2, pp. 53–78.

Takahashi, M., Hight, D. W., and Vaughan, P. R. (1980). “Effective stress changes observed during undrained cyclic triaxial tests on clay.” International Symposium on Soils under Cyclic and Transient Loading, Swansea, 7-11 January, 201–209.

Zhou, J., and Gong, X. N. (2001). “Strain degradation of saturated clay under cyclic loading.” Can. Geotech. J., 38, 208–212.